Published in final edited form as:
Mol Microbiol. 2010 July 1; 77(1): 236–251. doi:10.1111/j.1365-2958.2010.07207.x.

Interaction specificity, toxicity, and regulation of a paralogous set of ParE/RelE-family toxin-antitoxin systems

Aretha Fiebig[1,*], **Cyd Marie Castro Rojas**[1], **Dan Siegal-Gaskins**[2,§], and **Sean Crosson**[1,3,*]

[1]Department of Biochemistry and Molecular Biology, The University of Chicago, Chicago, IL, 60637

[2]Department of Physics, The University of Chicago, Chicago, IL, 60637

[3]The Committee on Microbiology, The University of Chicago, Chicago, IL, 60637

Summary

Toxin-antitoxin (TA) gene cassettes are widely distributed across bacteria, archaea, and bacteriophage. The chromosome of the α-proteobacterium, *Caulobacter crescentus*, encodes eight ParE/RelE-superfamily toxins that are organized into operons with their cognate antitoxins. A systematic genetic analysis of these *parDE* and *relBE* TA operons demonstrates that seven encode functional toxins. The one exception highlights an example of a non-functional toxin pseudogene. Chromosomally-encoded ParD and RelB proteins function as antitoxins, inhibiting their adjacently-encoded ParE and RelE toxins. However, these antitoxins do not functionally complement each other, even when overexpressed. Transcription of these paralogous TA systems is differentially regulated under distinct environmental conditions. These data support a model in which multiple TA paralogs encoded by a single bacterial chromosome form independent functional units with insulated protein-protein interactions. Further characterization of the *parDE*$_1$ system at the single-cell level reveals that ParE$_1$ toxin functions to inhibit cell division but not cell growth; residues at the C-terminus of ParE$_1$ are critical for its stability and toxicity. While continuous ParE$_1$ overexpression results in a substantial loss in cell viability at the population level, a fraction of cells escape toxicity, providing evidence that ParE$_1$ toxicity is not uniform within clonal cell populations.

Keywords

toxin-antitoxin; protein interaction; ParE; RelE; specificity; *Caulobacter*

Introduction

Bacterial toxin-antitioxin (TA) systems were initially identified on plasmids as genetic elements that promote stable plasmid inheritance (Gerdes *et al.*, 1985; Jaffe *et al.*, 1985). Typically contained in two-gene operons encoding an antitoxin protein followed by its cognate toxin, TA systems enhance plasmid stability in cell populations via post-segregational killing of plasmid-free daughters (Gerdes *et al.*, 1986; Jaffe *et al.*, 1985). The mechanistic basis of cell killing hinges on the differential stability of the antitoxin and toxin proteins. Specifically, the antitoxin is subject to a higher basal degradation rate. Cells failing to inherit the TA genes upon cell division are unable to replace proteolyzed antitoxin,

[*] To whom correspondence should be addressed: The University of Chicago, Department of Biochemistry and Molecular Biology, 929 E. 57th Street, GCIS W138, Chicago, IL 60637, 773-834-1926, scrosson@uchicago.edu.
[§]Current address: Mathematical Biosciences Institute, The Ohio State University, Columbus, OH.

resulting in inhibition of essential cellular processes by the free toxin. In this way, plasmid-free cells are arrested or killed (Lehnherr and Yarmolinsky, 1995; Tsuchimoto *et al.*, 1992; Van Melderen *et al.*, 1994).

While the role of select TA systems in the stable maintenance of plasmid or bacteriophage DNA is well documented (Gerdes *et al.*, 2005; Hayes, 2003; Jensen and Gerdes, 1995), the dramatic rise in publicly-available bacterial and archaeal genome sequences over the past decade has revealed thousands of examples of chromosomally-encoded TA gene pairs. These chromosomal toxins are contained within nine different phylogenetic groups, and function to inhibit either DNA replication or protein synthesis (Pandey and Gerdes, 2005). Among the most well-studied of the chromosomal systems is *relB-relE*, which has been implicated in cellular adaptation to environmental stress and nutrient limitation in *Escherichia coli* (reviewed in (Gerdes *et al.*, 2005; Van Melderen and De Bast, 2009). RelB-RelE TA systems are widely distributed, with operons annotated in the archaea, and both gram-positive and gram-negative bacteria (Anantharaman and Aravind, 2003; Makarova *et al.*, 2009; Pandey and Gerdes, 2005).

Included in a phylogenetic clade adjacent to the RelE family toxins are the ParE toxins (Anantharaman and Aravind, 2003). *parE*, along with its antitoxin *parD*, was first identified as a gene that conferred stability on the broad-host-range plasmid RK2 (Roberts and Helinski, 1992; Roberts *et al.*, 1994). While ParE toxin has significant primary sequence homology with RelE (see Fig. 1B), its cellular target is different. ParE inhibits gyrase and thereby blocks chromosome replication (Jiang *et al.*, 2002), and RelE inhibits translation by promoting cleavage of mRNA in the ribosomal A-site (Christensen and Gerdes, 2003; Neubauer *et al.*, 2009; Pedersen *et al.*, 2003). Chromosomal *parDE* TA systems are widespread within bacteria, and are abundant in γ-proteobacteria and in several species of α-proteobacteria (Anantharaman and Aravind, 2003; Pandey and Gerdes, 2005).

Although bacterial genomes often contain multiple copies of related TA genes, the function, regulation, and interactions between homologous TA proteins encoded from the same chromosome are not well understood. The chromosome of the α-proteobacterium, *Caulobacter crescentus*, encodes 8 RelE/ParE-family TA systems making it an ideal system to address these questions. Here we report a systematic analysis of toxin-antitoxin protein recognition and specificity among the four *parDE* and four *relBE* systems in *C. crescentus*. Our molecular genetic analysis of the full set of predicted *parDE* and *relBE* operons reveals that seven encode *bona fide* toxin-antitoxin protein pairs that exhibit exquisite specificity in toxin-antitoxin recognition: each toxin protein is inhibited only by its adjacently-encoded antitoxin. The one exception is *parDE*$_2$, which has acquired an apparent frameshift mutation that truncates the C-terminus of ParE$_2$ and renders it non-toxic. Transcriptional analysis indicates that these eight operons are independently and differentially regulated across multiple environmental conditions, providing evidence that paralogous TA systems are functionally distinct.

Using the *C. crescentus parDE*$_1$ operon as a model, we further characterize the toxicity and regulation of chromosomal *parDE* systems. In the absence of the ParD$_1$ antitoxin, ParE$_1$ is highly toxic to both *E. coli* and *C. crescentus*; transcription of the *parDE*$_1$ operon is autoregulated by the ParD$_1$ antitoxin, a regulatory feature commonly observed in TA systems. Serial truncation of ParE$_1$ demonstrates that residues at the extreme C-terminus of ParE$_1$ are necessary for protein stability and toxicity. Characterization of ParE$_1$ toxicity at the single cell level reveals that induction of ParE$_1$ toxin results in inhibition of cell division but not cell growth. Population level studies of toxicity demonstrate that while overexpression of ParE$_1$ toxin dramatically reduces culture growth and cell viability, a sub-

population of cells survives toxin overexpression and rapidly resumes growth upon attenuation of toxin expression.

Results

C. crescentus encodes seven functional ParE/RelE family TA systems and one pseudo-TA system

The genome of *C. crescentus* is predicted to contain four *parDE* and four *relBE* operons (Pandey and Gerdes, 2005); all exhibit the canonical operon structure of a 5′ antitoxin gene followed by a toxin gene (Fig. 1A & 1C). We used a reverse genetic approach to determine if these annotated toxin-antitoxin operons encode functional toxin-antitoxin protein pairs. Specifically, we attempted to create in-frame chromosomal deletions of each predicted 1) *parDE* and *relBE* operon, 2) *parE* and *relE* toxin gene, and 3) *parD* and *relB* antitoxin gene using a standard double recombination gene replacement strategy (see Fig. S1 for schematic) (Ried and Collmer, 1987). We successfully replaced each putative *parE* or *relE* toxin and *parDE* or *relBE* operon with truncated null alleles (Table 1) demonstrating that none of the eight toxin genes or toxin-antitoxin operons are essential under laboratory conditions. However, all attempts to replace the putative antitoxin genes $parD_1$, $parD_3$ or $parD_4$ and $relE_1$-$relE_4$ with null alleles failed (Table 1). Complementation of each of these antitoxin genes with a copy of the gene *in trans* on a replicating plasmid permitted deletion of chromosomal genes at expected frequencies (Tables 2 and 3). Together these data demonstrate that without simultaneous deletion of their cognate toxin genes, antitoxin genes are essential for cell viability. Thus, each operon encodes an antitoxin protein that protects the cell from its adjacently encoded toxin.

The one exception was the putative antitoxin $parD_2$. We successfully deleted the chromosomal copy of antitoxin $parD_2$ without *in trans* complementation (Table 1), demonstrating that $parD_2$ is not essential. Alignment of the adjacent $parE_2$ toxin gene to related toxin sequences revealed that it has acquired a mutation that introduces a premature stop codon near the C-terminus of the protein (Fig. 1B and Fig. S2). This stop codon results in a truncated $parE_2$ coding region that is approximately 20 codons shorter than the consensus ParE toxin sequence (COG3668) defined in the Conserved Domain Database (Marchler-Bauer and Bryant, 2004). Codons for conserved C-terminal residues remain intact 3′ of $parE_2$ stop codon, suggesting that this mutation occurred recently (Fig. S2). Previous studies of ParE toxin from plasmid RK2 have shown that C-terminal truncations attenuate protein toxicity (Roberts and Helinski, 1992). Based on this and additional C-terminal truncation data presented below, we propose that a nonsense or frameshift mutation in $parE_2$ ablates toxicity of the $ParE_2$ protein, thereby permitting deletion of the $parD_2$ antitoxin gene. As our data provide evidence that *C. crescentus* $parE_2$ encodes a non-functional toxin, we have reannotated this as a pseudogene operon, ψ-$parDE_2$.

Toxin-antitoxin pairs encoded from the same operon exhibit specific protein-protein recognition

The gene deletion data presented above provide evidence that each ParE and RelE toxin is uniquely bound and inhibited by the antitoxin encoded from its own operon. Specifically, the 0% deletion frequency for $parD_1$, $parD_3$, and $parD_4$ and $relB_1$-$relB_4$ (Table 1) demonstrates that endogenously-expressed ParD and RelB antitoxin proteins do not complement the loss of each other. The absence of endogenous complementation could either be due to 1) an inability of toxins and antitoxins encoded from non-adjacent positions to interact, or 2) insufficient levels of free endogenous antitoxin. To distinguish between these hypotheses, we attempted to systematically delete the essential $parD_1$, $parD_3$, and

$parD_4$ and *$relB_1$-$relB_4$* genes in the presence of a complete set of complementing overexpression plasmids.

Complementation of each *parD* and *relB* with a xylose-inducible copy of itself on a replicating plasmid permits chromosomal gene deletion at expected frequencies (Tables 2 and 3). However, chromosomal deletions of the *parD* and *relB* antitoxin genes were not recovered when any other antitoxin was overexpressed *in trans* (Tables 2 and 3). This lack of cross-complementation between the four *parD* and four *relB* antitoxins, even under conditions of overexpression, demonstrates that toxins and antitoxins encoded from non-adjacent chromosomal positions do not functionally interact.

These data support a model in which simultaneously expressed chromosomal TA systems exhibit a high degree of specificity between cognate toxin and antitoxin proteins (Fig. 1C). While these toxin proteins share ~20-30 % sequence identity, ParD and RelB antitoxin sequences are even less conserved (Fig. S3). This low level of sequence conservation combined with the observed genetic specificity suggests that each TA pair has co-evolved and constitutes an insulated genetic unit.

Transcription of toxin-antitoxin operons is differentially regulated

To assess the functional overlap between these related TA systems, we evaluated transcription of each operon under a range of conditions by transcriptional profiling or by using promoter fusions to *lacZ*. As toxin-antitoxin systems are known to be involved in stress response, we examined cells with and without a variety of stresses.

Excess heavy metals can cause oxidative stress by generating free radicals in the cytoplasm. Hu *et al.* (2005) examined the global transcriptional response of *C. crescentus* to chromium, cadmium, selenium and uranium. As expected, cellular response to these heavy metal stresses showed hallmarks of oxidative stress such as upregulation of superoxide dismutase, gluthathione S-transferase, thioredoxin and glutaredoxins (Hu *et al.*, 2005). Closer examination of *parDE* and *relBE* in these data sets revealed that both *ψ-$parDE_2$* and *$relBE_3$* operons are significantly upregulated by more than two fold in response to both chromate and dichromate salts (Fig. 2A and 2B; $p<0.005$; one sample t-test to determine if the mean Log_2(stressed/unstressed) is significantly different from 0, the expectation for an unregulated gene). Transcription of *$relBE_1$* is also increased in response to chromate and dichromate ($p< 0.01$), but by less than 2-fold. Transcription of *parDE* and *relBE* operons did not change significantly in response to cadmium (Fig. 2C) or selenium or uranium (not shown). Similarly, Hu *et al.* (2005) observed the strongest response in oxidative stress genes upon chromate and dichromate treatment suggesting that *ψ-$parDE_2$* and *$relBE_3$* are upregulated under conditions of strong oxidative stress. Alternatively, this response could be specific to chromate and dichromate.

To test if this was a general response to oxidative stress or a specific response to chromium stress, we exposed wild-type *C. crescentus* cells to 100 mM DETA-NONOate for 30 minutes. NONOate decomposition releases nitric oxide and thus is an alternative means to inducing oxidative stress. Transcriptional profiling of NONOate treated and untreated cells using a spotted oligo microarray revealed that *ψ-$parDE_2$* and *$relBE_3$* are uniquely upregulated among the *parDE* and *relBE* operons (Fig. 2D). This result suggests that regulation of *ψ-$parDE_2$* and *$relBE_3$* is a general response to oxidative stress. Transcriptional regulation of the *ψ-$parDE_2$* operon is somewhat surprising considering that the $ParE_2$ toxin is truncated. However, we take this as further evidence that the degeneration of *$parE_2$* is a relatively recent event.

To assess role of temperature stress on the activity of each of *parDE* and *relBE* promoter in wild-type cells, we fused approximately 500 bp upstream of each operon to *lacZ* and used β-galactosidase activity as a measure of promoter activity. Only one promoter, P_{relBE1}, was significantly ($p<0.0001$) activated by more than 2-fold at 37°C compared to 30°C (Fig. 2E). P_{parDE1}, P_{parDE3} and P_{parDE4} responded significantly ($p<0.0001$) to elevated temperatures, but to a much lesser extent. Notably, the TA operons regulated by temperature stress are distinct from those regulated by oxidative stress.

To assess the role of growth phase in regulation of the *C. crescentus parDE* and *relBE* genes, we monitored β-galactosidase activity from each promoter in early log (0.1 OD_{660}) and mid-log (0.3 OD_{660}) just before culture densities begin to deviate from exponential growth. This comparison revealed regulation of yet another set of TA operons (Fig. 2F). Transcriptional activity from $P_{\psi\text{-}parDE2}$, P_{relBE1} and P_{relBE2} increased more than 2-fold between early log and mid-log phase growth ($p<0.0001$). Activity of P_{parDE3} also increased significantly ($p<0.0001$), but by less than 2-fold.

Not all conditions tested elicited changes in transcription of *parDE* or *relBE* genes. Studies of TA systems in *Mycobacterium tuberculosis* have demonstrated that hypoxia induces expression of some TA loci (Ramage *et al.*, 2009). Transcriptional profiling of *C. crescentus* cells subjected to hypoxic stress revealed no significant changes in expression of *parE*/*relE* genes relative to unstressed cells (Fig. 2G). Similarly, transcription of these genes was not affected by the available nitrogen source in the growth medium; expression of *parDE* and *relBE* operons was unchanged between cells grown with either ammonium or nitrate as the sole nitrogen source (Fig 2H). Combined these data indicate that paralogous TA systems are not functionally redundant as they are activated under distinct environmental conditions.

C. crescentus $ParE_1$ and $ParD_1$ form an autoregulated toxin-antitoxin system

Among the ParD-ParE pairs encoded by *C. crescentus*, $ParD_1$ and $ParE_1$ are most similar to those encoded by the archetypal *parDE* system of plasmid RK2 (Fig. S3). Consequently, we chose to investigate *C. crescentus* $parDE_1$ as a model for chromosomally-encoded *parDE* TA pairs. Analysis of *parDE* from plasmid RK2 has shown that $parDE_{RK2}$ transcription is autorepressed by the $ParD_{RK2}$ antitoxin (Roberts *et al.*, 1993), which contains N-terminal ribbon-helix-helix DNA binding domain (Dalton and Crosson, 2010;Oberer *et al.*, 2002). To characterize transcriptional autoregulation of *C. crescentus* $parDE_1$, we monitored activity from a P_{parDE1}-*lacZ* fusion in wild-type ($parDE_1^+$) cells and in cells missing the toxin ($\Delta parE_1$) or the full operon ($\Delta parDE_1$). In wild-type cells, P_{parDE1} is moderately active during log phase growth (Fig. 3A). In a $\Delta parDE_1$ background, activity from P_{parDE1} is increased by approximately 2-fold, indicating repression in wild-type cells by either $ParD_1$ or the $ParD_1$-$ParE_1$ complex. In $\Delta parE_1$ cells, when all of the $ParD_1$ in the cell is unbound to toxin, P_{parDE1} promoter activity is even lower than wild type. This additional repression when $ParD_1$ is completely uncoupled from $ParE_1$ is small (~10%) but highly reproducible and statistically significant ($p<0.01$ by ANOVA and Tukey post test). Together these data indicate that $ParD_1$, either alone or in complex with $ParE_1$, negatively regulates transcription of $parDE_1$. Thus, like its RK2 homolog, the *C. crescentus* $parDE_1$ operon is autorepressed via the $ParD_1$ antitoxin (Fig. 3B).

Full-length $ParE_1$ is toxic to *E. coli* and *C. crescentus* at low concentrations

Repeated attempts to directionally clone full-length $parE_1$ into various expression plasmids in *E. coli* failed, implicating lethality from leaky expression of $parE_1$. All recovered clones contained insertion/deletion (indel) mutations in either the open reading frame or in the 5′ leader sequence (Fig. S4). As a result, isolated $parE_1$ clones were frameshifted or had a truncated ribosome binding site (RBS). The only successful means of generating a wild-type

full-length clone of *parE$_1$* in *E. coli* required co-expression of the antitoxin *parD$_1$*, either as a co-transcribed unit (pMT630-*parDE$_1$*) or from an independent promoter on the same plasmid (pETDuet-*parD$_1$-parE$_1$*; (Dalton and Crosson, 2010)). These results provide additional evidence that ParE$_1$ is a potent toxin that is neutralized by its antitoxin ParD$_1$.

Full-length *parE$_1$* was cloned into a low-copy vanillate-inducible expression plasmid, pMT630 (Thanbichler *et al.*, 2007); construction of this clone required deletion of six bases from the RBS (Fig. 4A). We denote this ΔRBS attenuated version of *parE$_1$* as *parE$_1$**. The effects of ParE$_1$ expression from pMT630-*parE$_1$** were assayed by quantifying the growth rate of a population in liquid culture. Expression from pMT630-*parE$_1$** in a wild-type genetic background has no effect on growth (Fig. 4B & 4C) demonstrating that endogenous ParD$_1$ antitoxin is sufficient to neutralize low levels of ParE$_1$ translated from a transcript with an attenuated RBS. In a *parDE$_1$* null background (Δ*parDE$_1$*), induction from pMT630-*parE$_1$** results in a 15% slower generation time than the empty vector control strain (148±7 minutes vs. 129±2 minutes; $p < 0.01$; Fig. 4B & 4C). Thus, in the absence of the cognate ParD$_1$ antitoxin, full-length ParE$_1$ affects the growth of *C. crescentus* cultures at low expression levels. Notably, coexpression of the complete TA pair from pMT630-*parDE$_1$* (with a wild-type RBS) has no effect on bulk growth (Fig. 4B & 4C).

ParE$_1$ C-terminal truncations attenuate protein toxicity and reduce protein stability

As attempts to assay the effects of *parE$_1$* expression on *C. crescentus* were confounded by problems cloning the gene, we sought to engineer variants of *parE$_1$* that had reduced toxicity. To this end, we created three *parE$_1$* C-terminal truncations that encode ParE$_1$(1-92), ParE$_1$(1-86), and ParE$_1$(1-79) (Fig. 1B & 4D). These mutants are missing 4, 10, and 17 residues from their C-termini, respectively. Unlike full-length *parE$_1$*, all three of these mutant toxins could be cloned into both pMT630 and pMT552 in *E. coli* and transformed into *C. crescentus* Δ*parDE$_1$* strains, indicating that these truncated gene products are less toxic than full-length ParE$_1$.

Expression of ParE$_1$(1-92) affects several aspects of growth in *C. crescentus* including initial doubling time in liquid culture and transition to stationary phase. Of the three truncated alleles, *parE$_1$(1-92)* is the only one that affects growth of wild-type cells. Vanillate-induced overexpression of ParE$_1$(1-92) slows the doubling of wild-type cells by 15% relative to an empty vector control strain (152±6 minutes vs. 132±2 minutes, $p < 0.001$; Fig. 4B & 4C). The toxicity of ParE$_1$(1-92) is accentuated in a Δ*parDE$_1$* background where growth is dramatically affected: culture doubling time is 80% slower than an empty vector control (doubling time of 239±33 minutes vs. 129±2 minutes; $p < 0.001$; Fig. 4C). Moreover, ParE$_1$(1-92) expression reduces the terminal density of the culture relative to empty vector controls in both wild-type and Δ*parDE$_1$* backgrounds (Fig. 4B). The apparent increase in ParE$_1$(1-92) toxicity in the absence of chromosomal *parDE$_1$* demonstrates that endogenous ParD$_1$ antitoxin partially neutralizes the effects of ParE$_1$(1-92) overexpression and that truncated ParE$_1$(1-92) is a potent inhibitor of growth.

The toxic effects of ParE$_1$(1-92) are greater than full-length ParE$_1$ (expressed from the *parE$_1$** plasmids) under equivalent inducing conditions. However, we note that expression from the plasmid bearing full-length ParE$_1$ is attenuated by a deletion of the RBS. Thus, the effects of ParE$_1$(1-92) and full-length ParE$_1$ expression under equivalent culture conditions cannot be directly compared due to differences in protein expression levels (see below). The fact that *parE$_1$(1-92)* can be directionally cloned in an expression plasmid in *E. coli* while the full length gene cannot implies that its toxicity has been somewhat attenuated.

Induction of ParE$_1$(1-86) has no effect on growth of *C. crescentus* in a Δ*parDE$_1$* background. Both initial growth rates and transition to stationary phase are statistically

similar to the empty vector control strain (Fig. 4B & 4C) indicating that the 10 C-terminal residues of $ParE_1$ are required for toxicity. In a wild-type background, induction of $ParE_1$(1-86) has no effect on initial doubling time, yet this strain consistently slows and exits from log phase before the empty vector control (Fig. 4B & 4C). This result suggests a model in which $ParE_1$(1-86) is inherently non-toxic but has the capacity to titrate $ParD_1$ antitoxin away from endogenous $ParE_1$, thereby increases the concentration of unbound, full-length $ParE_1$ in wild-type cells.

Overexpression of $ParE_1$(1-79), which is missing the last 17 residues from the C-terminus, has no effect on growth of wild-type or Δ*parDE*$_1$ cells (Fig. 4B & 4C) thus this truncation has rendered $ParE_1$ completely non-toxic. The non-toxic phenotype of this truncation supports our systematic gene deletion result showing that $ParE_2$, which is ~20 residues shorter than other ParE paralogs and is similar in length to $ParE_1$(1-79) (Fig 1B), no longer encodes a functional toxin.

One possibility to explain the lack of toxicity of $ParE_1$(1-79) and $ParE_1$(1-86) is that the last 17 or 10 residues of ParE are important for interactions with its cellular target. An alternate possibility is that these residues are important for the overall stability of the protein. The crystal structure of *C. crescentus* $ParE_1$ in complex with its $ParD_1$ antitoxin reveals significant secondary and tertiary structure in the 17 C-terminal residues (Fig. 1B & 4D) (Dalton and Crosson, 2010); thus it is likely that truncation of the C-terminus destabilizes the protein.

To assess protein stability, we tagged the N-terminus of each of the $ParE_1$ variants in pMT630 with a hemagglutinin (HA) epitope. Expression of the HA-tagged $ParE_1$ toxins was induced in wild-type cells. Tagged proteins were detected with anti-HA antibodies in a western blot (Fig. 4E). Induction from pMT630-*HA-parE*$_1$*(1-92)* resulted in robust accumulation of the toxin lacking the final 4 residues. However, HA-ParE1(1-86) was only weakly detectible and HA-ParE1(1-79) was completely undetectable (Fig. 4E). Thus deletion of the last 4 residues attenuates toxicity enough to permit cloning, however it does not significantly destabilize the toxin. Further truncations severely or completely destabilize and thereby inactiate the toxin. As expected, protein levels from the *HA-parE*$_1$* construct containing a truncated RBS are substantially lower than from the *HA-parE*$_1$*(1-92)* construct which contains a full-length RBS.

$ParE_1$ expression results in loss of viability in the culture population; surviving cells exhibit rapid recovery

To examine the effects of toxin on cell viability, we simultaneously monitored colony forming units (CFU) and optical density after induction of toxin alleles. Experiments were carried out in a Δ*parDE*$_1$ genetic background to eliminate interactions between plasmid-expressed toxins and endogenous $ParD_1$-$ParE_1$. To ensure uniform copy number throughout the population and to eliminate the possibility of plasmid free cells, toxin alleles were expressed from single-copy plasmids integrated at the *vanR* locus. In addition, after 5 hours of induction, we diluted the cells 10-fold to reduce the concentration of inducer and monitored recovery by optical density and CFU/ml.

When the *parE*$_1$* allele is continuously induced from a single copy locus (Δ*parDE*$_1$*vanR*::*pMT552-parE*$_1$*), initial growth measured by optical density is identical to the empty vector control and to cultures expressing the truncated, non-toxic $ParE_1$(1-86) protein; only in stationary phase is a difference observed (Fig. 5A). However, CFU monitoring revealed a 70% reduction in viability after 5 hours compared to control strains (Fig. 5B). Thus, even though density measurements indicate ‘normal’ growth, a large portion of cells expressing low levels of full-length toxin is incapable of forming colonies.

After 5 hours of induction and subsequent dilution, outgrowth of this population is slower, but eventually reaches optical densities and CFUs/ml comparable to the controls (Fig. 5C & 5D).

Congruent with what we observed during expression from multi-copy plasmids, induction of the truncated *parE$_1$(1-92)* allele, has more dramatic toxic effects than the *parE$_1$** alleles. Initially, the density of *C. crescentus* Δ*parDE$_1$vanR::pMT552-parE$_1$*(1-92) cultures increase at the same apparent rate as control strains, however the density increase stops abruptly after 8 hours of ParE$_1$(1-92) induction (Fig. 5A). This growth curve does not exhibit the expected logistic form, suggesting that the increase in culture density may be due to cell filamentation in the absence of cell division. Indeed, phase-contrast light microscopy after ParE$_1$(1-92) expression reveals elongated cells (Fig. 5E). Concomitant monitoring of CFUs shows that the number of viable cells rapidly decreases upon induction of ParE$_1$(1-92); there is a greater than 2-log loss in CFU within 2.5 hours. After 5 hours of expression, the number of culturable cells decreases by ~3 logs (Fig. 5B). This is the apparent limit for loss of viability under these conditions, as continued induction of ParE$_1$(1-92) does not further decrease CFUs (Fig. 5B). Thus, under these expression condition, continuous induction of ParE$_1$(1-92) results in death (or loss of culturability) of ~99.9% of the culture population, while 0.1% remain viable even with prolonged toxin induction.

While over 99% of cells overexpressing ParE$_1$(1-92) die or lose the ability to form colonies within 5 hours, a subset of cells in this culture have the capacity to rapidly resume growth after expression of ParE$_1$(1-92) is turned off. Specifically, 10-fold dilution of the culture with growth medium lacking inducer results in recovery of culture growth after 25 hours as monitored spectroscopically (Fig. 5C). Concomitant monitoring of CFUs upon dilution reveals a log-linear increase in colony number across a 3-log range within the same 25-hour period (Fig. 5D). The log linear increase in CFU suggests exponential growth of a subset of cells upon attenuation of induction.

Single-cell analysis of ParE$_1$ overexpression reveals inhibition of division but not cell growth

To assess the effect of ParE$_1$ toxin on individual *C. crescentus* cells, we utilized a single-cell culture and imaging assay previously described by our group (Siegal-Gaskins and Crosson, 2008). This method takes advantage of the natural capacity of *C. crescentus* to adhere to surfaces via the holdfast structure at the tip of the stalk (Fig. 6A). Using this microfluidic culture method, growth and division of cells under continuous flow of medium and constant concentration of inducer can be quantified. Specifically, parameters such as cell area, cell elongation rate, and cell division timing can be determined for single cells (see Fig. 6B). When toxic ParE$_1$ alleles were expressed from the replicating plasmid pMT630, we observed significant selection for plasmid free cells (Fig. S5). Therefore, to eliminate ambiguities caused by plasmid loss in these single-cell experiments, we analyzed the behavior of cells in which the inducible toxin gene was chromosomally integrated. Because the *parE$_1$** allele has a subtle effect on the behavior of bulk cultures in single-copy (Fig. 5), we compared the growth and division behavior of cells carrying the integrated *parE$_1$(1-92)* allele (CB15 Δ*parDE$_1$vanR::pMT552-parE$_1$(1-92)*) with empty vector control cells. After two hours of induction in a culture tube, cells were transferred to a microfluidic chamber and observed for 6 hours under continuous exposure to vanillate. Time-lapse movies are provided as supplemental material (Movie S1 and Movie S2).

Expression of ParE$_1$(1-92) in a Δ*parDE$_1$* background results in a dramatic reduction of cell division. Empty vector control cells divide at regular intervals (Fig. 6B) such that 75-80% of cells divide in each one-hour interval (Fig. 6C). Only 50% of toxin expressing cells divide within the first hour of observation, and the probability of observing a division event drops

to nearly 0% by the end of the experiment (Fig. 6C). However, this inhibition of cell division does not translate to inhibited cell growth. In fact, cells expressing toxin continue to elongate at rates comparable to or faster than control cells in the absence of cell division (Fig. 6B and 6D). This combination of normal to elevated growth combined with a reduction of cell division leads to elongated, filamentous cells (see Supplemental Movies S1-2) and explains the increase in optical density observed in bulk culture (Fig. 5A). Eventually, after 8 hours of continuous induction (i.e. 2 hours of induction prior, and 6 hours during observation in the microfluidic), growth begins to slow (Fig. 6D). This observation is congruent with what we observe in bulk culture: the increase in optical density stops abruptly after about 8 hours of continuous toxin induction (Fig. 5A).

Discussion

Chromosomal *parDE* / *relBE*-family TA operons encode insulated, autonomous protein complexes

The systematic analysis of *C. crescentus* ParDE / RelBE-family TA systems presented herein has shown that toxin-antitoxin interactions within a cell are restricted to those proteins that are encoded from directly adjacent positions on the chromosome. While the annotated toxin genes and full TA operons could be deleted, we were unable to delete the *parD* and *relB* antitoxin genes alone (with one exception involving toxin pseudogene $\psi parE_2$). This result indicates that each antitoxin gene is essential when its adjacent toxin gene remains intact and that related chromosomal antitoxins are not complementary at endogenous levels (Table 1). This interaction specificity is further evidenced by experiments in which we attempted to force cross-interaction between TA proteins encoded from non-adjacent chromosomal positions. Specifically, we assessed the full matrix of ParD-ParE and RelB-RelE interactions *in vivo* by quantifying how overexpression of each antitoxin gene affected the deletion frequency of each chromosomal antitoxin. For the seven essential *parD* and *relB* antitoxins, a chromosomal deletion was only possible when we expressed the deletion target from a plasmid (see Tables 2 and 3). Together, these results provide evidence for a model in which the chromosomal *parDE* and *relBE* operons of *C. crescentus* encode antitoxin and toxin proteins that interact specifically with their coexpressed operon partner and are insulated from interaction with other TA proteins.

While highly similar *ccdAB* TA systems have been observed to functionally interact (Saavedra De Bast *et al.*, 2008; Wilbaux *et al.*, 2007), the majority of TA systems investigated appear to show specificity for only their cognate partner. *In vivo* interactions were not detected between the related plasmid-encoded Axe-Txe TA system of pRUM and the chromosomally-encoded YefM-YoeB system of *E. coli* (Grady and Hayes, 2003); chromosomally-encoded YefM-YoeB homologues from *E. coli* and *Streptococcus pheumoniae* are incapable of cross-complementation (Nieto *et al.*, 2007); and a survey of subset of the *vapBC* paralogs in *Mycobacterium tuberculosis* showed functional interactions between only cognate toxin-antitoxin pairs (Ramage *et al.*, 2009). Likewise, our data demonstrate that paralogous TA systems encoded from the same bacterial chromosome are structurally insulated from cross-operon interactions. Thus, each of these evolutionarily-related TA modules are presumed to function autonomously.

Toxin-antitoxin cassettes and genome stabilization

It has been shown that chromosomal *parDE* and *relBE* TA systems can function to stabilize integron regions of bacterial chromosomes against deletion (Szekeres *et al.*, 2007). Bacterial integrons are mobile genetic platforms that can encode dozens of proteins, including TA systems, and have been implicated in the spread of antibiotic resistance among gram-negative pathogens (Mazel, 2006). While there is no apparent integron in *C. crescentus*, the

parDE and *relBE* operons in *C. crescentus* have several closely-related homologs within integrons of *V. cholerae* and other *Vibrionaceae*. Indeed, in the entire non-redundant protein database of GenBank, the most closely-related proteins to *C. crescentus* $ParE_1$ are encoded in *Vibrio* spp.

Our systematic *parDE/relBE* gene deletion data are inconsistent with an essential functional role for chromosomal TA systems in genome stabilization. In particular, we draw analogy between deletion of an entire TA operon and loss of a non-essential genomic region containing a TA operon. Our success in deleting all individual *parDE* / *relBE* TA operons from the *C. crescentus* chromosome demonstrates that none of the individual TA operons have the capacity to completely stabilize their respective chromosomal loci. Nonetheless, we cannot rule out the possibility that *parDE* and *relBE* gene cassettes reduce the probability of chromosomal DNA loss/reduction at the population level.

Differential regulation of TA transcription

Further evidence that chromosomal TA paralogs form independent functional units is evident in our analysis of TA gene transcription across a range of environmental stress and nutrient conditions. Specifically, we observe that the eight *parE*/*relE* operons are independently and differentially regulated across multiple environmental conditions. The high degree of congruence observed in the induction of ψ-$parDE_2$ and $relBE_3$ operons across both heavy metal- and nitric oxide-induced oxidative stress evidences a common activation mechanism underlying these systems that is triggered by the oxidative state of the cell. A distinct set of TA operons were regulated under heat shock and the transition from log phase to stationary phase growth, providing evidence for an alternative sensory and activation mechanism for transcription of these systems. Furthermore, we have demonstrated that environmental stressors known to activate transcription of other classes of TA systems in *M. tuberculosis* (e.g. hypoxia) (Ramage *et al.*, 2009) have no significant effect on the expression of ParE/RelE systems in *C. crescentus*.

A genetic determination of residues required for $ParE_1$ toxicity and $ParD_1$-$ParE_1$ binding

A series of $ParE_1$ mutants provide insight into residues that are required for cellular toxicity, protein stability and toxin-antitoxin interaction. Removing only 4 amino acids from the end of the toxin ($ParE_1$(1-92)) is sufficient to reduce toxicity without substantially affecting protein stability, while removing 17 amino acids ($ParE_1$(1-79)) completely ablates stability and toxicity. The effects of these mutations on protein stability are not surprising in light of the recent crystal structure of the $ParD_1$-$ParE_1$ complex (Dalton and Crosson, 2010). While truncation of the last 4 amino acids in the $ParE_1$(1-92) mutant reduces toxicity, it is not predicted to significantly perturb the secondary or tertiary structure of the protein. Conversely, deletion of the 17 C-terminal amino acids of the protein in $ParE_1$(1-79) removes an entire β-strand from the structure, which renders the protein wholly unstable (see Fig. 4).

The mutant protein $ParE_1$(1-86), which is missing 10 residues from its C-terminus, has significantly reduced stability relative to $ParE_1$ and $ParE_1$(1-92). This mutant also has differential toxicity when it is overexpressed in a wild-type versus a Δ$parDE_1$ genetic background. In a wild-type background, $ParE_1$(1-86) expression results in slowed growth after the culture reaches mid-log phase (Fig. 4A). However, there is no apparent effect of expressing this same construct in a genetic background in which the chromosomal $parDE_1$ operon has been deleted (Fig. 4B and Fig. 5). We interpret these results as evidence that the last 10 residues of $ParE_1$ are essential for protein toxicity, but that $ParE_1$(1-86) still has the capacity to interact with chromosomally-expressed $ParD_1$ antitoxin and titrate it away from endogenous $ParE_1$. Thus, $ParE_1$(1-86) is not inherently toxic but retains some capacity to interact with $ParD_1$, thereby causing secondary toxic effects.

Fractional cell survival and adaptation to environmental stress

Another proposed function for chromosomal TA systems is that they serve to mediate adaptation and survival during environmental stress conditions (reviewed in (Gerdes *et al.*, 2005; Van Melderen and De Bast, 2009)). In the case of *E. coli mazEF*, it has been proposed that TA system activation results in programmed cell death within a fraction of a population (Engelberg-Kulka *et al.*, 2006); fractional death is believed to sustain the surviving cells by supplying nutrients. A competing model for *mazEF* and *relBE* function in *E. coli* is that these TA systems do not induce cell death, but rather have a bacteriostatic function during stress / starvation (Christensen *et al.*, 2001; Christensen *et al.*, 2003). The data presented in this paper demonstrate that overexpression of $ParE_1$(1-92) inhibited cell division and reduced the capacity of *C. crescentus* to form colonies on solid media by ~3 log units relative to an empty vector control strain (Fig. 5 and 6). We do not know whether the decrease in CFUs upon $ParE_1$ overexpression was due to cell death or was a result of cells entering a viable but non-culturable state. Loss of viability / culturability upon continuous overexpression of $ParE_1$(1-92) quickly reaches a plateau: CFUs do not decrease beyond 3 log units even though the culture clearly stops growing and dividing. Thus in the absence of $ParD_1$ antitoxin, induction of $ParE_1$ results in growth arrest, yet ~0.1% of the cells enter a static state that can be recultured on fresh nutrient agar. Moreover, we observed a rapid recovery of growth when we turned off expression of the $ParE_1$ toxin that was consistent with exponential growth. Our data do not definitively distinguish between a programmed cell death model and a bacteriostatic model for $ParD_1$-$ParE_1$ in *C. crescentus*. Under native conditions, where cells have the capacity to produce antitoxin, it is possible that activation of the toxin may be modulated such that cells primarily enter a static rather than cidal state. Experiments aimed at understanding the physiological mechanisms that activate the ParE toxins in the cell will help to distinguish between these models.

Experimental Procedures

Growth and culture conditions

E. coli strains used for cloning were cultured under standard conditions. Liquid cultures were grown in LB media (Fisher Scientific) and colonies were grown on LB + 1.5 % agar at 30° or 37° C supplemented with antibiotics as appropriate at the following concentrations: kanamycin 50 μg/ml, chloramphenicol 20 μg/ml, tetracycline 12 μg/ml.

C. crescentus strain were grown in peptone-yeast extract (PYE) or on PYE-agar plates (15 g agar/L) at 30° C (Ely, 1991) unless otherwise noted. Antibiotics were used at the following concentrations: kanamycin 5 μg/ml liquid media, 25 μg/ml solid media; chloramphenicol 1-2 μg/ml; tetracycline 1-2 μg/ml.

Growth curves—Overnight liquid cultures were inoculated from independent colonies and grown in 5 ml PYE in 20 mm glass tubes, in triplicate. These cultures were diluted to 0.05 OD in 2 ml fresh PYE in 13 mm tubes and incubated in an Infors tube shaker (ATR Biotech, Laurel, MD), at 30°C, 220 rpm. Cultures were induced with 500 μM vanillate (Thanbichler *et al.*, 2007) and optical density measurements at 660 nm were taken for individual cultures in a Genesys20 Spectrophotometer (ThermoFisher Scientific, Waltham, MA) every 40 or 50 minutes depending on the experiment. Additional vanillate was added every 2.5 hours to replace the vanillate metabolized by the cells. Antibiotics to select for plasmid maintenance were included in overnight as well as outgrowth conditions. The growth rate was determined by fitting the data from the first 4 hours of growth to an exponential growth equation: $y(t)= y_0e^{kt}$ in Prism (GraphPad Software, San Diego, CA), where y_0 is the initial cell density, k is growth rate, and t is time. Doubling time is 0.69 / k.

CFU—Colony forming units were determined by generating serial dilutions of each culture, and stamping 3 ul of each dilution onto PYE-agar plates using a replica plater (R2383, Sigma-Aldrich, St. Louis, MO). Each dilution was stamped in triplicate. Colonies were counted in dilutions exhibiting 3 to 30 colonies per stamp.

Microfluidic growth—Single-cell growth and division assays were conducted as described in (Siegal-Gaskins and Crosson, 2008) except that 500 μM vanillate was added to the media flowing through the channel. Briefly, overnight cultures were inoculated from individual colonies growing on a PYE-agar plate. Cells were diluted to an OD_{660} of 0.1 in fresh PYE containing 500 μM vanillate, outgrown for 2 hours, loaded into the microfluidic chamber and incubated for 30 min at 30°C before imaging. During imaging, PYE containing vanillate was flowed through the growth chamber at a constant flow rate of 20 μl / s with a PHD2000 infuser (Harvard Apparatus, Holliston, MA). Temperature in the room was maintained at 30°C. Cells were imaged with a DM5000 microscope (Leica, Wetzlar, Germany) at 630× magnification in phase-contrast mode. Images were collected at 2-min intervals on an Orca-ER digital camera (Hamamatsu, Hamamatsu City, Japan) for 6 hours per experiment. Light dosage was limited to 200 msec exposure and ~5 s manual focus time per exposure. Data on strains FC447 and FC1030 was collected in two independent experiments each.

Microfluidic division arrest and growth rate data analysis

For each experiment, 100 cells were chosen at random from the fields of view at the top of every hour and monitored for division during the period of the following hour. To calculate the single cell growth rate 10 cells were monitored in each experiment and the total cumulative cell area was used; cell area 'lost' during each division was added back as an offset to the measured area for the remainder of the experimental run. Whereas the 'true' cell area over time has a characteristic sawtooth shape, the cumulative area is a monotonically increasing function. The growth rate for each cell was then calculated by fitting the cumulative cell area data measured in every hour to a straight line. Growth rates for each interval were normalized to the average growth rate during the first hour of each experiment.

ImageJ (NIH, Bethesda, MD) was used for image processing, cell counting and cell area determination. Additonal data analysis and processing was done with Mathematica (Wolfram Research, Inc., Champaign, IL).

Cloning and strain construction

General PCR and subcloning—Specific regions of the *C. crescentus* genome were amplified from colonies using KOD hot-start polymerase (EMD Biosciences / Novagen). Reactions were supplemented with 5% DMSO. Restriction sites for cloning into target plasmids were added to the ends of the primers (see Table S2 for primer sequences). PCR products were ligated into pCR-BLUNT II-TOPO (Invitrogen, Carlsbad, CA) following manufacturers instructions. Sequences of the cloned products were confirmed. These pCR-blunt based plasmids were used for further sub-cloning into target plasmids using standard restriction digestion (enzymes from NEB, Ipswich, MA), gel purification (GeneJet Gel Extraction Kit, Fermentas, Glen Burnie, MD) and ligation (T4 DNA ligase, NEB, Ipswich, MA) following manufacturers protocols. The ΔRBS pMT552-$parE_1$* plasmid was constructed by subcloning P_{van}-ΔRBS-$parE_1$ from pMT630-$parE_1$*. Ligation products were transformed into TOP10 cells (Invitrogen, Carlsbad, CA) and plated on selective media. Inserts were verified by PCR and direct sequencing. Desired plasmids were transformed into *C. crescentus* strains by electroporation (Ely, 1991) or tri-parental mating (Ely, 1991) using FC3 as a helper strain (Table S1).

In-frame gene deletion—*C. crescentus* strains carrying gene deletions were constructed using a double recombination strategy (see Fig. S1 for schematic) (Ried and Collmer, 1987). Briefly, approximately 500 base pair regions flanking the 5′ and 3′ regions of the gene to be deleted were directionally ligated into the suicide plasmid pNPTS138. This plasmid carries *nptI* to select for integrants with kanamycin and *sac*B for counterselection on sucrose. pNPTS138-derived deletion plasmids were transformed into *C. crescentus* by electroporation and primary integrants were selected on PYE-Kan plates. Overnight growth in non-selective liquid media followed by plating on PYE-3% sucrose allowed identification of clones in which the plasmid had been excised in a second recombination event. PCR was used to confirm chromosomal deletions. Boarders of the deletion constructs can be determined from the primers used to amplify the 5′ and 3′ regions (see Table S2). Strains used for complementation also carried the replicating plasmid pMT686 with an antitoxin gene under the control of the P_{xyl} promoter. In these experiments, 0.3% xylose was added during non-selective growth and sucrose counter selection to ensure synthesis of the complementing antitoxin.

N-terminal HA fusions—Insertion of HA-tag coding sequence at the 5′ end of *$parE_1$* coding sequence was accomplished using overlap extension PCR (Higuchi *et al.*, 1988) using pMT630-based *$parE_1$* plasmids as the template. First the regions upstream and downstream of the site of insertion were amplified with primers that contained partial and overlapping sequences for the HA-tag at the 3′ end of the upstream fragment and the 5′ end of the downstream fragment. Then 1 μl of each of these reactions were mixed and used as the template for a second round of PCR using the extreme upstream and downstream primers to generate a single PCR product in which the 5′ and 3′ fragments are fused with the HA-coding sequence in between. The products amplified contained restrictions sites that are unique in the pMT630 sequence (AscI and NheI). Both pMT630 and the HA-containing PCR products were digested with AscI and NheI, gel purified and ligated together to generate pMT630-based plasmids bearing HA-parE_1 alleles. The sequences of all plasmids were confirmed.

Western blot analysis

Overnight cultures were diluted to 0.05 OD_{660} in fresh PYE and allowed to outgrow for 3 hours. Expression of HA-ParE_1 was then induced with the addition of 500 μM vanillate. After 2.5 hours of induction cells were harvested from 1.5 ml of culture and stored at -80°C. The OD_{660} of all genotypes was 0.30 +/- 0.015 at the time of harvest. Cells were resuspended in 40 μl of 3× protein loading buffer and boiled for 10 minutes. The proteins in 10 μl of each sample were separated using a 4-20% gradient SDS-tris-glycine polyacrylamide gel (Lonza, Basel Switzerland). Proteins were transferred to P^{sq}-Immobilon PVDF membrane (Millipore, Bedford MA) following manufacturers protocol for wet-transfer. The membrane was blocked with 5% dry milk for at least 1 hour. HA-tagged proteins were detected with a 1:2500 dilution of purified monoclonal mouse anti-HA antibodies (H3663, Sigma-Aldrich, St. Louis, MO). Simultaneously, as a loading control, the membrane was incubated with a 1:10,000 dilution of polyclonal rabbit anti-FixJ (CC_0758) antibodies. After 3 washes, the blot was incubated with a 1:2,500 dilution of goat anti-mouse antibodies conjugated to HRP (Thermo Scientific, Rockford, IL) and 1:10,000 HRP conjugated goat anti-rabbit antibodies (Thermo Scientific, Rockford, IL). After 5 washes, the secondary antibody was detected with SuperSignal West Femto Substrate (Thermo Scientific, Rockford, IL). Blots were exposed to film for 1-5 minutes.

Measuring transcriptional activity

Quantifying the transcriptional effects of hypoxic stress by Affymetrix GeneChip—To test the effects of hypoxic stress on TA transcription in *C. crescentus*, we

cultured strain CB15 in a New Brunswick bioreactor under controlled conditions. Prior to innoculation, the medium was bubbled with laboratory air at maximum flow and stirred at 300 rpm for 2 hours. After this period, the medium was considered saturated with air and the oxygen probe was set to 100%. Untreated cultures were grown in air-saturated complex medium at 30°C to OD_{660}=0.5 at pH=7 (continuous air-bubbling; 300 rpm stirring). At cell harvest in aerated culture, the dissolved oxygen probe remained above 98%. To subject cells to hypoxia, culture at OD_{660}=0.5, pH=7 was sparged continuously with nitrogen gas; the dissolved oxygen level as measured by the gas probe dropped from 100% to 0% over the course of 5 minutes under this condition. Hypoxic cultures were continually stirred and bubbled with nitrogen for another 20 minutes after the dissolved gas probe read 0%. Hypoxic cells were then harvested for RNA isolation. In both cases, RNA was isolated and purified as previously described (Boutte *et al.*, 2008). Two biologically independent samples were collected for each condition.

RNA integrity was checked on a Bioanalyzer (Agilent, Santa Clara, CA). Ten μg of each total RNA was processed to produce single-strand cDNA and RNA was removed using 1N NaOH. cDNA was column purified, fragmented using DNAseI (GE Life Sciences, Piscataway, NJ), and end labeled using GeneChip labeling reagent (Affymetrix, P/N 900542). Labeled cDNA was hybridized to GeneChip CauloHi1 according to GeneChip Expression analysis technical manual (Affymetrix, Santa Clara, CA). After hybridization for 16 hours at 50°C, arrays were washed using protocol PRO-GE-W52-V3 and stained on a GeneChipFluidics Station (Affymetrix) according to the Genechip Expression analysis technical manual. The arrays were scanned using the Affymetrix Gene Chip Scanner 3000 7G and CEL intensity files were generated by GCOS (Gene Chip Operating Software) v. 1.4. Hypoxia microarray data are deposited in the GEO database (http://www.ncbi.nlm.nih.gov/geo) under series accession GSE21127.

Quantifying the transcriptional effects of oxidative stress and nitrogen metabolism using spotted oligonucleotide arrays—To test the effects of oxidative stress on TA transcription (as elicited by nitric oxide treatment), six independent cultures of *C. crescentus* NA1000 were grown in PYE medium at 30°C to OD_{660}=0.3. 100 mM DETA-NONOate (Cayman Chemical, Ann Arbor, MI) was added to three of the rolled cultures for 30 minutes, while the other three cultures remained in the roller untreated. After this 30-minute treatment period, cultures were spun at 10,000× g for 30 seconds, the supernatant was removed, and the cell pellets were flash frozen in liquid nitrogen.

To test the effects of alternative nitrogen metabolism on TA expression, *C. crescentus* NA1000 cells were cultured in M2 glucose minimal medium containing either NH_4Cl as the sole nitrogen source as previously described (Ely, 1991) or 10 mM $NaNO_3$ as the sole nitrogen source. For each nitrogen condition, 4 replicate cultures were grown to OD_{660}=0.3–0.4. Cells were harvested at 10,000× g for 30 seconds, the supernatant was removed, and the cell pellets were flash frozen in liquid nitrogen. RNA was isloated and purified as previously described (Boutte *et al.*, 2008). RNA quality was assessed via agarose gel electrophoresis and RNA concentration determined by UV spectrophotometry using a Shimadzu UV-1650 (Shimadzu Scientific Instruments, Columbia, MD).

For oligo array quantification, labeled indodicarbocyanine-dCTP (Cy3) and indocarbocyanine-dCTP (Cy5) cDNA was generated from 20 μg of total RNA by reverse transcription with Superscript II reverse transcriptase (Invitrogen, Carlsbad, CA) using 1 μg of random hexamer primers (Invitrogen, Carlsbad, CA). Samples of cDNA from each RNA type (NONOate treated vs. untreated or NH_4^+ vs. NO_3^-) were either Cy3 labeled or Cy5 labeled. Dye-swapped cDNA was generated in order to minimize dye bias in the microarray analysis. Paired Cy3 and Cy5 labeled cDNA from samples were hybridized onto spotted

DNA oligo arrays using a protocol previously described (Hottes *et al.*, 2004). After hybridization and washing, the arrays were scanned with a GenePix 4000B scanner (Axon Instruments). Scanned spots were converted to ratios (red/green) with GenePix Pro 5.0 software. Expression ratio data for the four biological replicates were normalized by median centering. DNA microarray data for the NONOate treated versus untreated cells have been deposited in the Gene Expression Omnibus (GEO) database (http://ncbi.nlm.nih.gov/geo) under series accession GSE21139. Array data for NH_4^+ versus NO_3^- treated cells have been deposited in GEO under series accession GSE21203.

B-galactosidase promoter reporter assays—Approximately 500 bp upstream of each *parDE or relBE locus* was cloned into pPR9TT (Santos *et al.*, 2001) or pRKlac290 (Gober and Shapiro, 1992) upstream of *lacZ*. pPR9TT does not have a translation initiation site thus the resulting plasmids were translational fusions between the beginning of each antitoxin and *lacZ*. The pRKlac290-P_{parDE1} construct is a transcriptional fusion. β-galactosidase activity was determined colorimetrically; Z-buffer (60 mM Na_2HPO_4, 40 mM NaH_2PO_4, 10 mM KCl, 1 mM $MgSO_4$) and an excess of o-nitrophenyl-β-D-galactopyranoside were added to chloroform-permeabilized cells and absorbance was measured at 420 nm on a Spectronic Genesys 20 Spectrophotometer (ThermoFisher Scientific, Waltham, MA). Miller units are calculated using the following equation: MU=(A_{420} of reaction*1000) / (A_{660} of cells*t*v), where t = reaction time in minutes and v = volume of cells used in ml.

Supplementary Material

Refer to Web version on PubMed Central for supplementary material.

Acknowledgments

We thank members of the Crosson Lab for helpful discussions and Melissa Marks for a critical reading of the manuscript. pMT plasmids were a gift of Martin Thanbichler at MPI-Marburg. We thank the Shapiro and McAdams Labs at Stanford University for assistance with spotted array data collection. Construction of microfludic devices was supported by the NSF MRSEC facility at The University of Chicago. C-M.C.R. was supported by a Post-Baccalaureate Research Education Program (PREP) grant to The University of Chicago from NIH-NIGMS. S.C. acknowledges support for this project from the Arnold and Mabel Beckman Foundation (BYI) and the Mallinckrodt Foundation.

Literature Cited

Anantharaman V, Aravind L. New connections in the prokaryotic toxin-antitoxin network: relationship with the eukaryotic nonsense-mediated RNA decay system. Genome Biol. 2003; 4:R81. [PubMed: 14659018]

Boutte CC, Srinivasan BS, Flannick JA, Novak AF, Martens AT, Batzoglou S, Viollier PH, Crosson S. Genetic and computational identification of a conserved bacterial metabolic module. PLoS Genet. 2008; 4:e1000310. [PubMed: 19096521]

Christensen SK, Mikkelsen M, Pedersen K, Gerdes K. RelE, a global inhibitor of translation, is activated during nutritional stress. Proc Natl Acad Sci USA. 2001; 98:14328–14333. [PubMed: 11717402]

Christensen SK, Gerdes K. RelE toxins from bacteria and Archaea cleave mRNAs on translating ribosomes, which are rescued by tmRNA. Mol Microbiol. 2003; 48:1389–1400. [PubMed: 12787364]

Christensen SK, Pedersen K, Hansen FG, Gerdes K. Toxin-antitoxin loci as stress-response-elements: ChpAK/MazF and ChpBK cleave translated RNAs and are counteracted by tmRNA. J Mol Biol. 2003; 332:809–819. [PubMed: 12972253]

Dalton KM, Crosson S. A conserved mode of protein recognition and binding in a ParD-ParE toxin-antitoxin complex. Biochemistry. 2010; 49:2205–2215. [PubMed: 20143871]

Ely B. Genetics of *Caulobacter crescentus*. Meth Enzymol. 1991; 204:372–384. [PubMed: 1658564]

Engelberg-Kulka H, Amitai S, Kolodkin-Gal I, Hazan R. Bacterial programmed cell death and multicellular behavior in bacteria. PLoS Genet. 2006; 2:e135. doi:110.1371/journal.pgen.0020135. [PubMed: 17069462]

Gerdes K, Larsen JEL, Molin S. Stable inheritance of plasmid R1 requires two different loci. J Bacteriol. 1985; 161:292–298. [PubMed: 2981804]

Gerdes K, Rasmussen PB, Molin S. Unique type of plasmid maintenance function: postsegregational killing of plasmid-free cells. Proc Natl Acad Sci USA. 1986; 83:3116–3120. [PubMed: 3517851]

Gerdes K, Christensen SK, Lobner-Olesen A. Prokaryotic toxin-antitoxin stress response loci. Nat Rev Microbiol. 2005; 3:371–382. [PubMed: 15864262]

Gober JW, Shapiro L. A developmentally regulated Caulobacter flagellar promoter is activated by 3′ enhancer and IHF binding elements. Mol Biol Cell. 1992; 3:913–926. [PubMed: 1392079]

Grady R, Hayes F. Axe-Txe, a broad-spectrum proteic toxin-antitoxin system specified by a multidrug-resistant, clinical isolate of *Enterococcus faecium*. Mol Microbiol. 2003; 47:1419–1432. [PubMed: 12603745]

Hayes F. Toxins-antitoxins: plasmid maintenance, programmed cell death, and cell cycle arrest. Science. 2003; 301:1496–1499. [PubMed: 12970556]

Higuchi R, Krummel B, Saiki RK. A general method of in vitro preparation and specific mutagenesis of DNA fragments: study of protein and DNA interactions. Nucleic Acids Res. 1988; 16:7351–7367. [PubMed: 3045756]

Hottes AK, Meewan M, Yang D, Arana N, Romero P, McAdams HH, Stephens C. Transcriptional Profiling of Caulobacter crescentus during Growth on Complex and Minimal Media. J Bacteriol. 2004; 186:1448–1461. [PubMed: 14973021]

Hu P, Brodie EL, Suzuki Y, McAdams HH, Andersen GL. Whole-genome transcriptional analysis of heavy metal stresses in Caulobacter crescentus. J Bacteriol. 2005; 187:8437–8449. [PubMed: 16321948]

Jaffe A, Ogura T, Hiraga S. Effects of the ccd function of the F plasmid on bacterial growth. J Bacteriol. 1985; 163:841–849. [PubMed: 3897195]

Jensen RB, Gerdes K. Programmed cell death in bacteria: proteic plasmid stabilization systems. Mol Microbiol. 1995; 17:205–210. [PubMed: 7494469]

Jiang Y, Pogliano J, Helinski DR, Konieczny I. ParE toxin encoded by the broad-host-range plasmid RK2 is an inhibitor of *Escherichia coli* gyrase. Mol Microbiol. 2002; 44:971–979. [PubMed: 12010492]

Lehnherr H, Yarmolinsky MB. Addiction protein Phd of plasmid prophage P1 is a substrate of the ClpXP serine protease of *Escherichia coli*. Proc Natl Acad Sci USA. 1995; 92:3274–3277. [PubMed: 7724551]

Makarova KS, Wolf YI, Koonin EV. Comprehensive comparative-genomic analysis of type 2 toxin-antitoxin systems and related mobile stress response systems in prokaryotes. Biol Direct. 2009; 4:19. [PubMed: 19493340]

Marchler-Bauer A, Bryant S. CD-Search: protein domain annotations on the fly. Nucleic Acids Research. 2004; 32:327–331.

Mazel D. Integrons: agents of bacterial evolution. Nat Rev Microbiol. 2006; 4:608–620. [PubMed: 16845431]

Neubauer C, Gao YG, Andersen KR, Dunham CM, Kelley AC, Hentschel J, Gerdes K, Ramakrishnan V, Brodersen DE. The structural basis for mRNA recognition and cleavage by the ribosome-dependent endonuclease RelE. Cell. 2009; 139:1084–1095. [PubMed: 20005802]

Nieto C, Cherny I, Khoo SK, de Lacoba MG, Chan WT, Yeo CC, Gazit E, Espinosa M. The yefM-yoeB toxin-antitoxin systems of Escherichia coli and Streptococcus pneumoniae: functional and structural correlation. J Bacteriol. 2007; 189:1266–1278. [PubMed: 17071753]

Oberer M, Zangger K, Prytulla S, Keller W. The anti-toxin ParD of plasmid RK2 consists of two structurally distinct moieties and belongs to the ribbon-helix-helix family of DNA-binding proteins. Biochem J. 2002; 361:41–47. [PubMed: 11743881]

Pandey DP, Gerdes K. Toxin-antitoxin loci are highly abundant in free-living but lost from host-associated prokaryotes. Nucleic Acids Res. 2005; 33:966–976. [PubMed: 15718296]

Pedersen K, Zavialov AV, Pavlov MY, Elf J, Gerdes K, Ehrenberg M. The bacterial toxin RelE displays codon-specific cleavage of mRNAs in the ribosomal A site. Cell. 2003; 112:131–140. [PubMed: 12526800]

Ramage HR, Connolly LE, Cox JS. Comprehensive functional analysis of Mycobacterium tuberculosis toxin-antitoxin systems: implications for pathogenesis, stress responses, and evolution. PLoS Genet. 2009; 5:e1000767. [PubMed: 20011113]

Ried JL, Collmer A. An *nptI-sacB-sacR* cartridge for constructing directed, unmarked mutations in gram-negative bacteria by marker exchange-eviction mutagenesis. Gene. 1987; 57:239–246. [PubMed: 3319780]

Roberts RC, Helinski DR. Definition of a minimal plasmid stabilization system from the broad-host-range plasmid RK2. J Bacteriol. 1992; 174:8119–8132. [PubMed: 1459960]

Roberts RC, Spangler C, Helinski DR. Characteristics and significance of DNA binding activity of plasmid stabilization protein ParD from the broad host-range plasmid RK2. J Biol Chem. 1993; 268:27109–27117. [PubMed: 8262949]

Roberts RC, Strom AR, Helinski DR. The *parDE* operon of the broad-host-range plasmid RK2 specifies growth inhibition associated with plasmid loss. J Mol Biol. 1994; 237:35–51. [PubMed: 8133518]

Saavedra De Bast M, Mine N, Van Melderen L. Chromosomal toxin-antitoxin systems may act as antiaddiction modules. J Bacteriol. 2008; 190:4603–4609. [PubMed: 18441063]

Santos PM, Di Bartolo I, Blatny JM, Zennaro E, Valla S. New broad-host-range promoter probe vectors based on the plasmid RK2 replicon. FEMS Microbiol Lett. 2001; 195:91–96. [PubMed: 11167001]

Siegal-Gaskins D, Crosson S. Tightly regulated and heritable division control in single bacterial cells. Biophys J. 2008; 95:2063–2072. [PubMed: 18469083]

Szekeres S, Dauti M, Wilde C, Mazel D, Rowe-Magnus DA. Chromosomal toxin-antitoxin loci can diminish large-scale genome reductions in the absence of selection. Mol Microbiol. 2007; 63:1588–1605. [PubMed: 17367382]

Thanbichler M, Iniesta AA, Shapiro L. A comprehensive set of plasmids for vanillate- and xylose-inducible gene expression in *Caulobacter crescentus*. Nucleic Acids Res. 2007; 35:e137. [PubMed: 17959646]

Tsuchimoto S, Nishimura Y, Ohtsubo E. The stable maintenance system *pem* of plasmid R100: degradation of PemI protein may allow PemK protein to inhibit cell growth. J Bacteriol. 1992; 174:4205–4211. [PubMed: 1624414]

Van Melderen L, Bernard P, Couturier M. Lon-dependent proteolysis of CcdA is the key control for activation of CcdB in plasmid-free segregant bacteria. Mol Microbiol. 1994; 11:1151–1157. [PubMed: 8022284]

Van Melderen L, De Bast MS. Bacterial toxin-antitoxin systems: more than selfish entities? PLoS Genet. 2009; 5:e1000437. doi:1000410.1001371/journal.pgen.1000437. [PubMed: 19325885]

Wilbaux M, Mine N, Guerout AM, Mazel D, Van Melderen L. Functional interactions between coexisting toxin-antitoxin systems of the ccd family in Escherichia coli O157:H7. J Bacteriol. 2007; 189:2712–2719. [PubMed: 17259320]

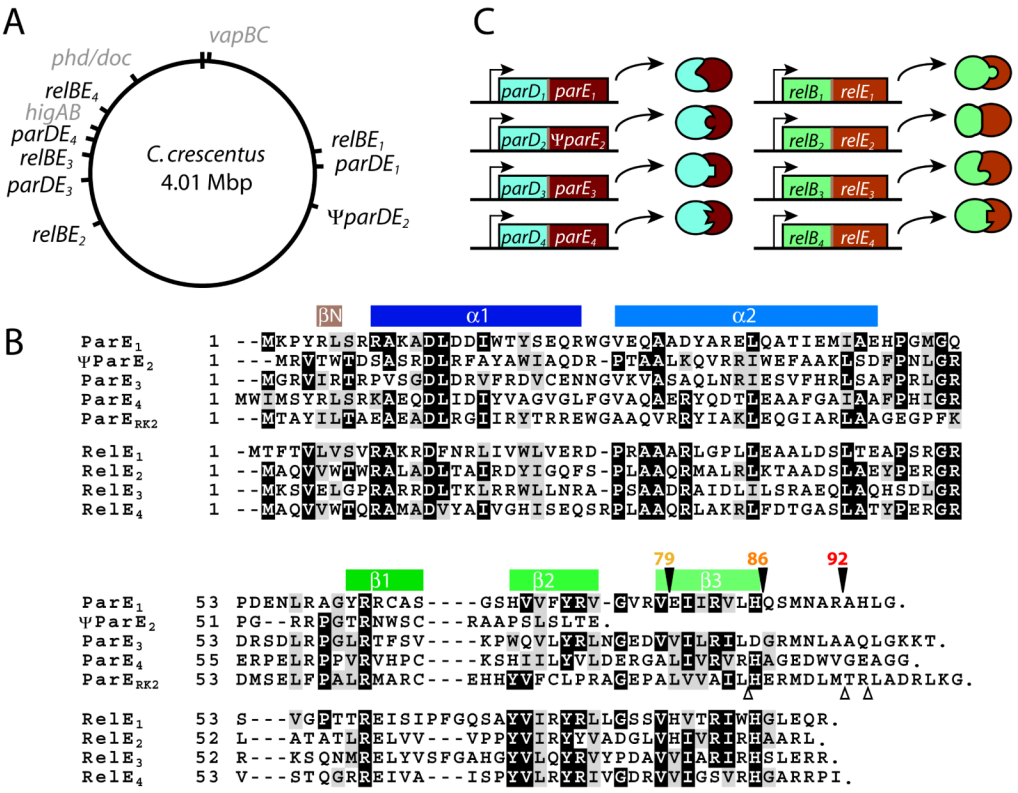

Fig. 1.

The *C. crescentus* genome encodes eight toxins in the ParE/RelE superfamily. **A.** The genomic positions of predicted toxin-antitoxin operon in the *C. crescentus* genome (Pandey and Gerdes, 2005). *parE* or *relE* homologs are black; other TA families are grey. *oriC* is at the top of the circle **B.** ClustalW alignment of ParE/RelE homologues from *C. crescentus* and the plasmid RK2 (Larkin *et al.*, 2007). Residues that are similar or identical in 60% of the sequences are shaded in grey or black, respectively. Colored bars indicate secondary structure elements defined in the $ParE_1$ crystal structure (Dalton and Crosson, 2010). Filled triangles above $ParE_1$ indicate the sites of C-terminal truncations engineered in this study. Open triangles below $ParE_{RK2}$ indicate truncations that prevent this toxin from stabilizing plasmids (Roberts and Helinski, 1992). **C.** Schematic representation of simultaneous expression of multiple ParD-ParE and RelB-RelE pairs, each with unique interaction interfaces resulting in insulated, protein-protein complexes.

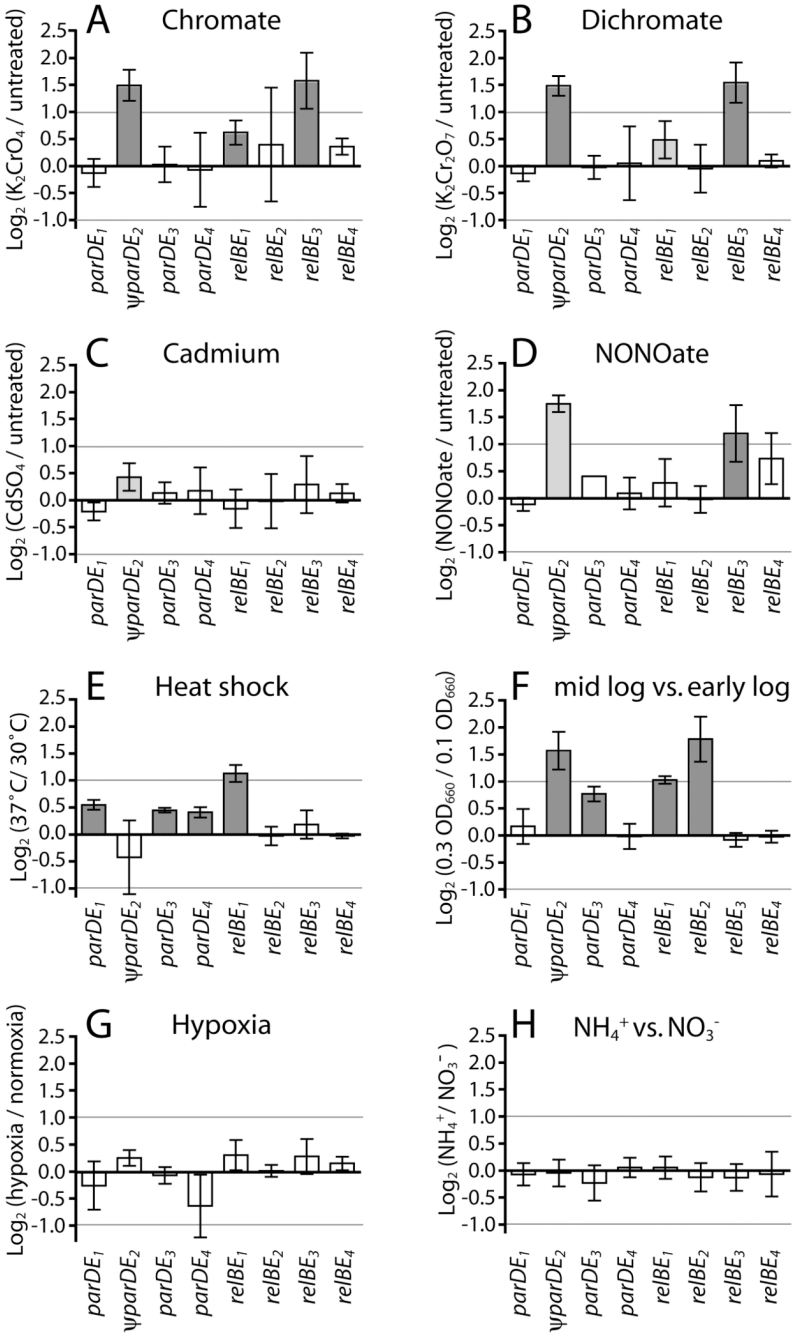

Fig. 2.

Expression of *parE*/*relE*-family TA systems is differentially regulated under distinct conditions. Expression of each operon was measured in pairs of conditions by Affymetrix GeneChip (**A-C** (Hu *et al.*, 2005) and **G**), spotted oligo array (**D** and **H**) or promoter fusion to *lacZ* (**E-F**). The ratio of expression between conditions was $\log_2$ transformed and the mean (+/- standard deviation) is presented. Filled bars indicate means significantly different from 0 (one sample t-test); $p<0.005$ dark gray, $p<0.05$ light gray. Microarrays were conducted in duplicate to quadruplicate (see methods) and values for both genes in the operon were averaged; β-galactosidase activities were measured in paired cultures on three

independent days (n=6). Light lines indicate two-fold differences in expression (log_2 expression ratio = +/-1).

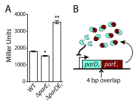

Fig. 3.

$ParD_1$ represses transcription of *parDE*$_1$. **A.** The promoter of *parDE*$_1$ was fused to *lacZ* in the plasmid pRKLac290. β-galactosidase activity was measured as a proxy for transcriptional activity from this promoter in wild-type, Δ*parE*$_1$ and Δ*parDE*$_1$ cells. Cultures were grown in PYE to early log phase (mean +/- SEM, n=6). Significance was assessed using 1-way ANOVA and Tukey post-test; * $p< 0.01$, ** $p< 0.001$. **B.** Model representing the auto-repressor activity of $ParD_1$. *parDE*$_1$ operon is shown indicating the 4 bp overlap between *parD*$_1$ and *parE*$_1$.

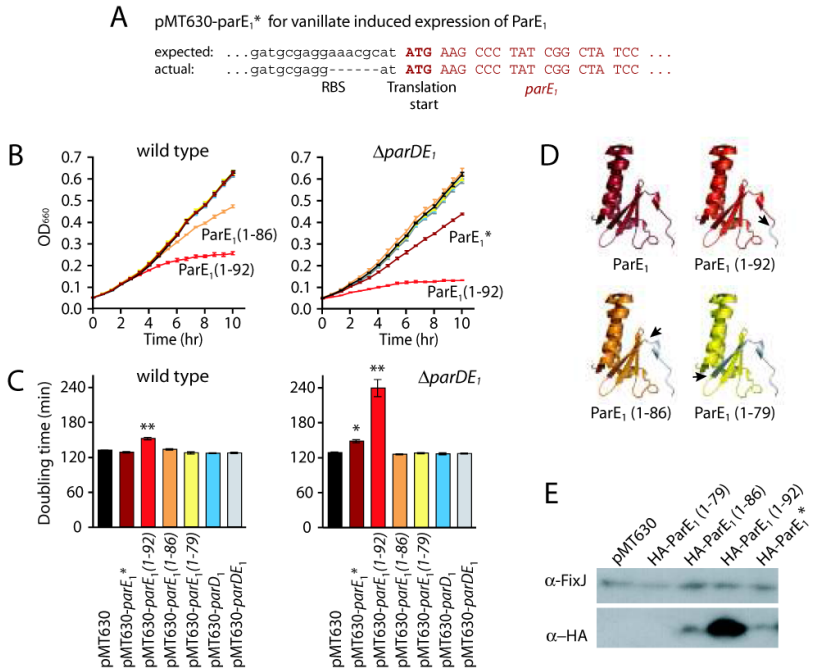

Fig. 4.

Expression of $ParE_1$ from the multi-copy plasmid pMT630 impairs growth; C-terminal truncations affect toxicity and stability of $ParE_1$. Components of the *parDE1* operon were expressed from pMT630, a low-copy, vanillate-inducible expression plasmid, in wild-type or Δ*parDE1* cells. **A.** Cloning of the full-length *parE1* gene required truncation of the ribosome binding site in pMT630. Plasmid and *parE1* gene sequences are in black and red respectively. Bases missing in the constructed plasmid are indicated by dashes. **B.** Growth of cultures in PYE supplemented with vanillate was monitored by optical density (mean +/- SEM; n=6). Colors are as in C; genotypes that differ from the empty vector control are labeled. **C.** Doubling time of each culture was calculated from the first 4 hours of growth and averaged (+/- SEM). Means were compared using 1-way ANOVA and Tukey post-test; * $p< 0.05$, ** $p< 0.001$. **D.** Ribbon diagram of $ParE_1$ monomer structure (Dalton and Crosson, 2010). Sites of C-terminal truncations are indicated by arrows and deleted portions of the sequence are shown in grey. **E.** Western blot of lysate from wild-type cells expressing N-terminally tagged HA-$ParE_1$ variants from pMT630. Anti-FixJ (CC_0758) antibodies were used to confirm equal loading of lysate in each lane.

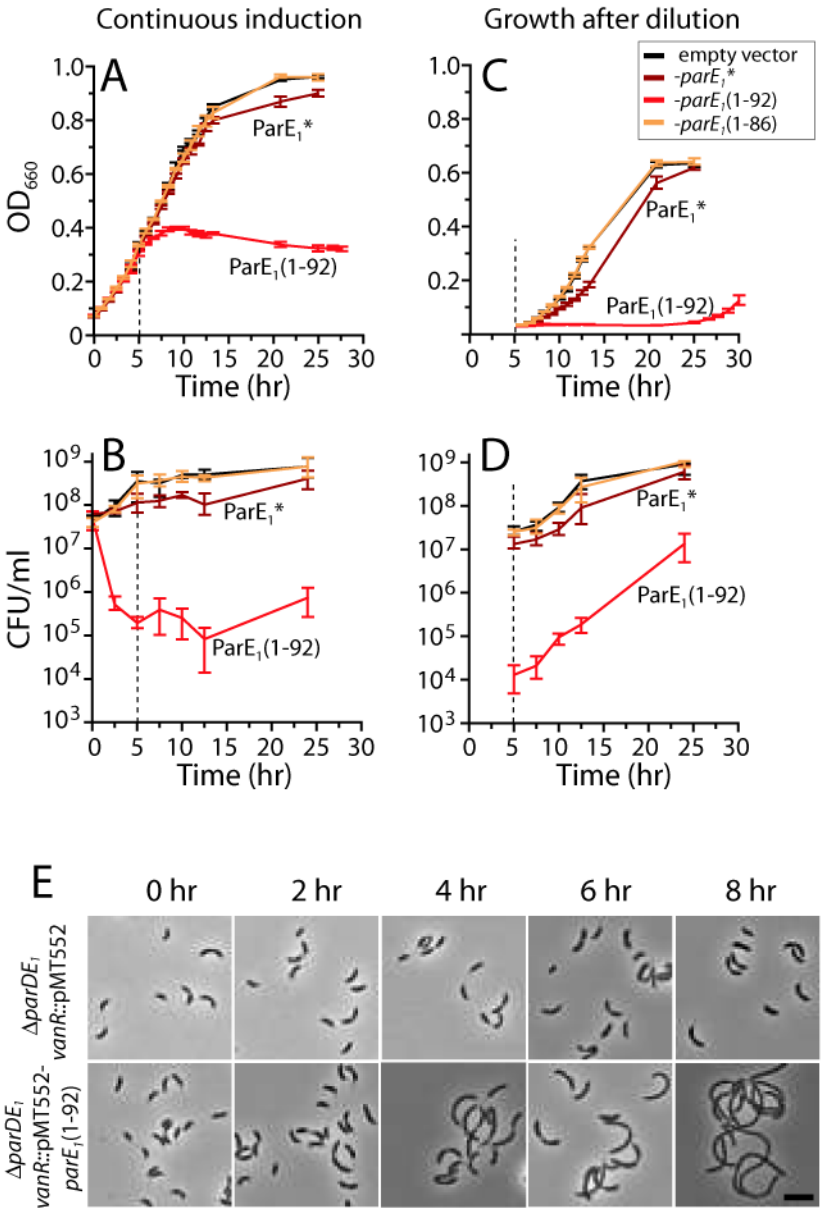

Fig. 5.

Overexpression of toxin results in a rapid loss of viability and filamentation in Δ*parDE*$_1$ cells. **A & B.** Growth and viability of cultures expressing chromosomally-integrated single-copy *parE1* alleles were monitored by optical density every 50 minutes and CFU/ml every 2.5 hours. To ensure continuous induction as vanillate is metabolized, cultures were spiked with additional vanillate every 2.5 hours for the first 12.5 hours. **C & D.** After 5 hours of induction, as the ParE$_1$(1-92) cultures reach a point of arrest, an aliquot of each culture was diluted 10-fold to dilute inducer (vertical dotted line). Recovery of the diluted cells was monitored by optical density and CFU/ml. Data is averaged from 4 independent cultures. Error bars represent SEM in A and C, and represent the range in B and D. **E.** Phase contrast images of empty vector control cells (top) and *parE*$_1$*(1-92)* expressing cells (bottom) captured throughout the course of induction. Scale bar in lower right image is 5 μm.

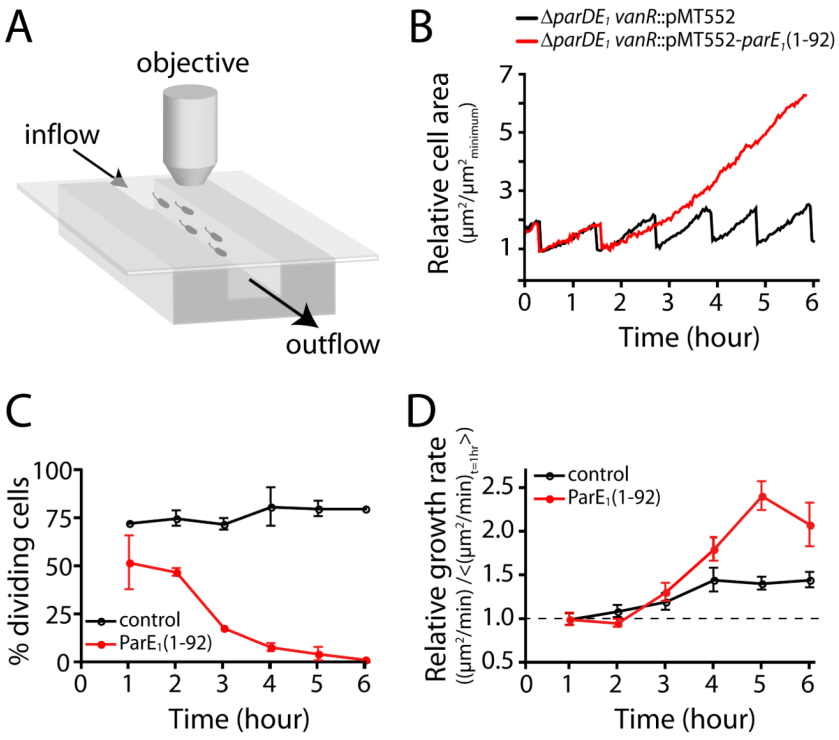

Fig. 6.

Single cell analysis of Δ*parDE*$_1$ cells expressing ParE$_1$(1-92) reveals division arrest, but not growth arrest. **A.** Schematic of the microfluidic growth chamber used to observe cell growth (adapted from (Siegal-Gaskins and Crosson, 2008)). *C. crescentus* cells adhere to the glass coverslip via the holdfast and are continuously bathed with fresh media (PYE) containing 500 μM vanillate. **B.** Cell area vs. time of a growing and dividing empty vector control cell (black) and a cell expressing *parE*$_1$*(1-92)* from the *vanR* locus (red). Abrupt decreases in cell area in the sawtooth trace indicate cell division. **C.** Percent of cells that divide in a 1-hour interval; mean (+/- SEM) from two independent experiments with each genotype is presented. **D.** Growth rate (+/- SEM) of individual cells normalized to mean growth rate during the first hour of each experiment (mean +/- SEM; n=20 cells per genotype). See methods for description of growth rate calculation.

Table 1

Deletion statistics for the full genomic set of *parDE* and *relBE* operons, individual *parD* and *relB* antitoxin genes, and *parE* and *relE* toxin genes in *C. crescentus*

Operon	Genbank locus tag numbers		Deletion target					
	strain CB15	strain NA1000	operon		toxin		antitoxin	
			null	WT	null	WT	null	WT
$parDE_1$	CC_0873-4	CCNA_00916-7	17	11	22	9	0	168
$parDE_2$	CC_1054†	CCNA_01106-7	5	34	19	82	62	87
$parDE_3$	CC_2756†	CCNA_02843-4	27	27	9	11	0	79
$parDE_4$	CC_2984-5	CCNA_03079-80	8	38	9	40	0	134
$relBE_1$	CC_0802-3	CCNA_00844-5	28	18	21	18	0	59
$relBE_2$	CC_2513-4	CCNA_02598-9	16	32	20	29	0	54
$relBE_3$	CC_2879-80	CCNA_02973-4	27	33	23	21	0	64
$relBE_4$	CC_3131†	CCNA_03231-2	29	55	9	21	0	47

† Sequences corresponding to $parE_2$, $parD_3$ and $relB_4$ are present in the published genome sequence of *C. crescentus* strain CB15 (Nierman, et al., 2001), but were not annotated as genes.

Table 2

Deletion statistics for the essential *C. crescentus parD* antitoxin genes in the presence of a complementing copy of each *parD*

Complementing plasmid	Deletion target					
	***parD*$_1$**		***parD*$_3$**		***parD*$_4$**	
	null	**WT**	**null**	**WT**	**null**	**WT**
pMT686-*parD*$_1$	70	18	0	39	0	48
pMT686-*parD*$_2$	0	48	0	73	0	67
pMT686-*parD*$_3$	0	62	25	57	0	60
pMT686-*parD*$_4$	0	65	0	65	26	58

Table 3

Deletion statistics for the *C. crescentus relB* antitoxin genes in the presence of a complementing copy of each *relB*

Complementing plasmid	Deletion target							
	***relB*$_1$**		***relB*$_2$**		***relB*$_3$**		***relB*$_4$**	
	null	**WT**	**null**	**WT**	**null**	**WT**	**null**	**WT**
pMT686-*relB*$_1$	16	24	0	68	0	95	0	47
pMT686-*relB*$_2$	0	88	34	41	0	75	0	89
pMT686-*relB*$_3$	0	81	0	90	36	54	0	94
pMT686-*relB*$_4$	0	77	0	43	0	90	17	31